BNL-94046-2010-CP

Long Range Active Detection of HEU Based on Thermal Neutron Multiplication

L. Forman, I. Dioszegi, C. Salwen, and P.E. Vanier

Presented at SORMA XII – 2010 Symposium on Radiation Measurements and Applications
Ann Arbor, Michigan
May 24-27, 2010

September 2010

Nonproliferation and National Security Department

Brookhaven National Laboratory

U.S. Department of Energy
Department of Homeland Security, DOE - Office of Science

Notice: This manuscript has been authored by employees of Brookhaven Science Associates, LLC under Contract No. DE-AC02-98CH10886 with the U.S. Department of Energy. The publisher by accepting the manuscript for publication acknowledges that the United States Government retains a non-exclusive, paid-up, irrevocable, world-wide license to publish or reproduce the published form of this manuscript, or allow others to do so, for United States Government purposes.

This preprint is intended for publication in a journal or proceedings. Since changes may be made before publication, it may not be cited or reproduced without the author's permission.

DISCLAIMER

This report was prepared as an account of work sponsored by an agency of the United States Government. Neither the United States Government nor any agency thereof, nor any of their employees, nor any of their contractors, subcontractors, or their employees, makes any warranty, express or implied, or assumes any legal liability or responsibility for the accuracy, completeness, or any third party's use or the results of such use of any information, apparatus, product, or process disclosed, or represents that its use would not infringe privately owned rights. Reference herein to any specific commercial product, process, or service by trade name, trademark, manufacturer, or otherwise, does not necessarily constitute or imply its endorsement, recommendation, or favoring by the United States Government or any agency thereof or its contractors or subcontractors. The views and opinions of authors expressed herein do not necessarily state or reflect those of the United States Government or any agency thereof.

Long Range Active Detection of HEU Based on Thermal Neutron Multiplication

L. Forman[1], I. Dioszegi[2*], C. Salwen[2] and P. E. Vanier[2]

[1]Ion Focus Technology, Miller Place, New York 11764
[2]Brookhaven National Laboratory, Upton, New York 11973.
[*]Corresponding author, email: dioszegi@bnl.gov, Tel: (631) 344 7020

Abstract

We report on the results of measurements of proton irradiation on a series of targets at Brookhaven National Laboratory's (BNL) Alternate Gradient Synchrotron Facility (AGS), in collaboration with LANL and SNL. We examined the prompt radiation environment in the tunnel for the DTRA-sponsored series (E 972), which investigated the penetration of air and subsequent target interaction of 4 GeV proton pulses. Measurements were made by means of an organic scintillator with a 500 MHz bandwidth system.

We found that irradiation of a depleted uranium (DU) target resulted in a large gamma-ray signal in the 100-500 μsec time region after the proton flash when the DU was surrounded by polyethylene, but little signal was generated if it was surrounded by boron-loaded polyethylene. Subsequent Monte Carlo (MCNPX) calculations indicated that the source of the signal was consistent with thermal neutron capture in DU. The MCNPX calculations also indicated that if one were to perform the same experiment with a highly enriched uranium (HEU) target there would be a distinctive fast neutron yield in this 100-500 μsec time region from thermal neutron-induced fission. The fast neutrons can be recorded by the same direct current system and differentiated from gamma ray pulses in organic scintillator by pulse shape discrimination.

Keywords: Spallation, thermal neutrons, fast neutrons, fission, pulse shape discrimination, high band width data recording.

1. Introduction

The radiation pulse time response of fast photomultiplier (PM)/scintillators makes it possible to record high count rates, 10^7 c/s. However, when the PM is operated at high gain, these devices are actually count rate limited by the bleeder strings that supply charge to the PM dynode structure. It is possible to operate the PM at low gain where the charge per particle may be a factor of 1/1000 lower such that the inter-dynode charge can be replaced between particles. We have used this technique for measurements of gamma ray and neutron spectroscopy on BNL AGS E-972 experimental series where targets were exposed to single proton pulses of duration <100ns containing 10^{11} protons in a pulse.

2. High bandwidth data recording and spectroscopy

The proton flash produced many thousands of gamma rays incident on the scintillator. Initially, the detector output signal (measured at the anode) reached the PM saturation voltage or the highest voltage the anode circuit can deliver. Moreover, the high current in all the later dynodes drew charge from its capacitive storage at a rate not replaceable by the bleeder string. This caused a gain reduction that was fixed until charge replacement occurred from the high voltage supply through the bleeder string. The time of flight neutron signal followed the proton flash, after 0.1-1.0 μsec. The neutron current signal was usually quite low and there is no evidence that it further discharged the PM dynode structure. The recovery of gain occurred ~150 μsec after the proton flash. We were able to estimate the PM gain during the neutron time of flight signal from the PM recovery signal. The neutron spectra derived from the cross-section measurement data using the estimated gain was in agreement with theory.

After gain recovery, analysis of the recorded data was performed by counting pulses within a chosen time and amplitude window. Pulse height was converted into deposited gamma ray energy based on Co-60 calibration with the detector in position in the AGS experiment tunnel.

2. Experimental spectra and data analysis

In our experiment the prompt gamma and neutron radiation was detected using a liquid organic scintillator (Bicron 501A, 5 inches diameter x 2 inch thick) in direct current mode using a 500 MHz digital recording system. After detector recovery from the intense prompt gamma and neutron signal, individual pulses from nuclear interactions could be recorded. The time resolution was 10 ns over 200 ms recorded time range. The recording was triggered by the accelerator pulse. The gain of the PM was set to be about 10^{-3} of normal high gain. Fig. 1. displays a full recorded data set from 0 to 200 ms and also shows (as an insert) a ~10 μs long section of the recorded data at higher resolution.
[PLACE OF FIGURE 1]

It appears as though individual pulses are not resolved, but this is an artifact of photographic reproduction. The insert of Fig. 1. shows that at $2 \cdot 10^6$counts/sec that the recording resolution gives separable radiation pulses and that indicates that baseline noise is not very important. The full width at half maximum (FWHM) of the gamma-ray pulses was 15 ns. From the pulse height distribution, it is possible to derive the gamma-ray energy spectra as a function of time from the proton flash.

2.1 Cross section measurements

In the first phase of the experiment ("cross section measurements") different targets (thickness: ~18 g/cm^2) were irradiated by the 4 GeV proton pulses and the detector was placed at ~12m distance upstream. After the proton burst the first large observable peak in the detector is mainly from prompt gamma radiation. After the prompt peak the fast neutrons arrive (both initially formed by spallation and fission, or multiplied chain reactions). In this < 1μs region the fast neutrons are detected. In the following 1 μs to 0.2 s (the recorded time limit) the gamma-ray emission from the isomeric states of the spallation/fission products dominate. β-decay of the products should also be observable at later times (>0.1s).

We analyzed the isomeric transition region gamma-ray energy spectra of different targets by placing ~100 μs wide time windows and extracting the pulse height distribution within each window. An example of spectra, where the 100 μs window was started 350μs after the prompt burst is shown in Figure 2. [PLACE OF FIGURE 2] The liquid scintillator detector spectra are dominated by Compton scattering in the detector. The distinct observable feature is the Compton edge for each level. According to the measurement the highest gamma-ray energies are emitted from the products of U-235/238 irradiation. The poor energy resolution of the liquid scintillator prevents the identification of the target based on the gamma-ray data in the 350-450 μs time region, but the data suggest that the high energy photons may be an important indicator of the presence of uranium.

2.2 Measurements on bulk target and shielding materials

The second phase of the experiment was comparative to a 20 kg cube of DU in various configurations to test the ability of using this prompt recording technique to identify the DU targets in various shielding scenarios. The target station was placed at 10 or 20 m from our detector located in a tunnel where the beam passed 2 m from our detector (placed near the tunnel wall) on its way to the target assembly.

In the new configuration the bulk target was surrounded by different neutron and gamma-ray shielding materials. This produced some important, new effects. Most important of these is in the 100-500 μsec time region after the proton pulse: we observed an increased gamma-ray yield in the case of polyethylene shielding around DU, which disappears in the case where the polyethylene is boron loaded. This finding could be explained as follows. Fast spallation neutrons produced by the proton flash will undergo fast multiplication as they traverse fissionable material in the target. This will occur in all materials whose fission threshold is above 1.5 MeV (e.g. U-238). A fraction of the neutrons will be thermalized in the surrounding media. This results in the increased gamma-ray yield in the polyethylene, whereas the thermal neutrons are absorbed in the boron loaded polyethylene, and few gamma rays are produced in the time region 200-500 μs. The enhanced gamma-ray production is observable in Figure 3., where the measured average detector current plotted as a function time for different target configurations. In the 100-500 μs region the photo multiplier gain significantly recovered, but the high rate pulses pile up and create a baseline shift proportional to the gamma-ray energy times gamma-ray rate. This creates a current on the 50 Ω resistor of the oscilloscope. The measured quantity is the base line deviation in mV, averaged over 100 μs time. This is being plotted in Figure 3 for different target and shielding combinations. To verify these explanations and to extrapolate our measurements for HEU we performed Monte Carlo (MCNPX) calculations. [PLACE OF FIGURE 3]

4. Monte Carlo calculations

In the initial model calculations we investigated the time evolution of the system after a fission event generates a ~2 MeV fission neutron. To realize this scenario we started off with a 2 MeV neutron source placed in 20 kg U-235/238, and tallied the resulting neutron and gamma-flux.

We calculated the yield of fast and thermal neutrons in 100 μs steps in DU and HEU with and without polyethylene shield. The MCNPX calculations (Fig. 4.) indicated that if the target were highly enriched uranium (HEU) there would be a distinctive fast neutron yield in this 100-500 μsec time region from thermal-neutron induced fission. Our liquid scintillator detector and high bandwidth data recording system is capable of recording these fast neutrons and their pulses can be sorted out from the recorded mixed neutron and gamma-ray pulses in organic scintillator by off line pulse shape discrimination.[1]
[PLACE OF FIGURE 4]

5. Conclusion

We have measured the radiation output from a single pulse of 4 GeV protons incident on various targets. Although not described in this paper, we found all cross section targets (C, O-18, Al, Cu, Fe, Ni, Ti, Au, Pb, U-235, U-238) produced neutrons with spectra consistent with a Maxwellian kinetic temperature of the order of 1.5 MeV. The spallation and fission processes produced gamma emitting nuclides indicative of isomeric transitions. It was found that the presence of these nuclides were slowly varying with atomic mass (e.g., for iron and nickel) in agreement with many high energy proton measurements [2] in which that the charge distribution of spallation products was found to have a maximum close to the unchanged charge distribution quantity of the nuclear collision, (Z+1)/(A+1). However, U-235 and U-238 products had the highest energy photon production of the nuclides in our target set.

We found that in the presence of an efficient thermalizing material, e.g., polyethylene, there was a large gamma-ray signal. MCNP calculations suggest that these are from thermal neutron capture. MCNP calculations further suggest that thermal neutron fission in U-235 would produce high energy neutrons that would unequivocally separate HEU from DU. These data suggest that useful signatures can be obtained from moderated HEU using high energy proton irradiation, in a time window close to the prompt signal of the excitation pulse.

References

1. G.F. Knoll, Radiation Detection and Measurement, 3rd ed. New York: John Wiley &Sons, Inc., 2000, pp. 679-680.
2 P. Kozma and J. Kliman, “Spallation of nickel by 9 GeV/c protons and deuterons,” J. Phys. G: Nucl. Part. Phys. **16**, 45-53, (1990).

FIGURES

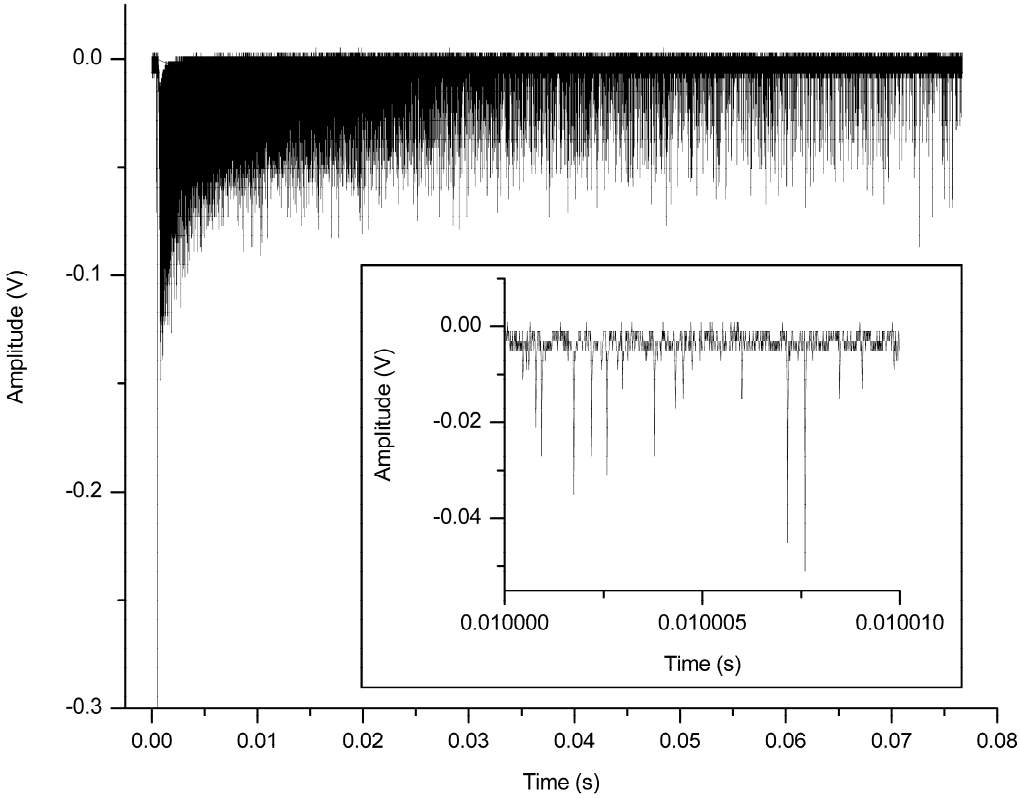

Figure 1.

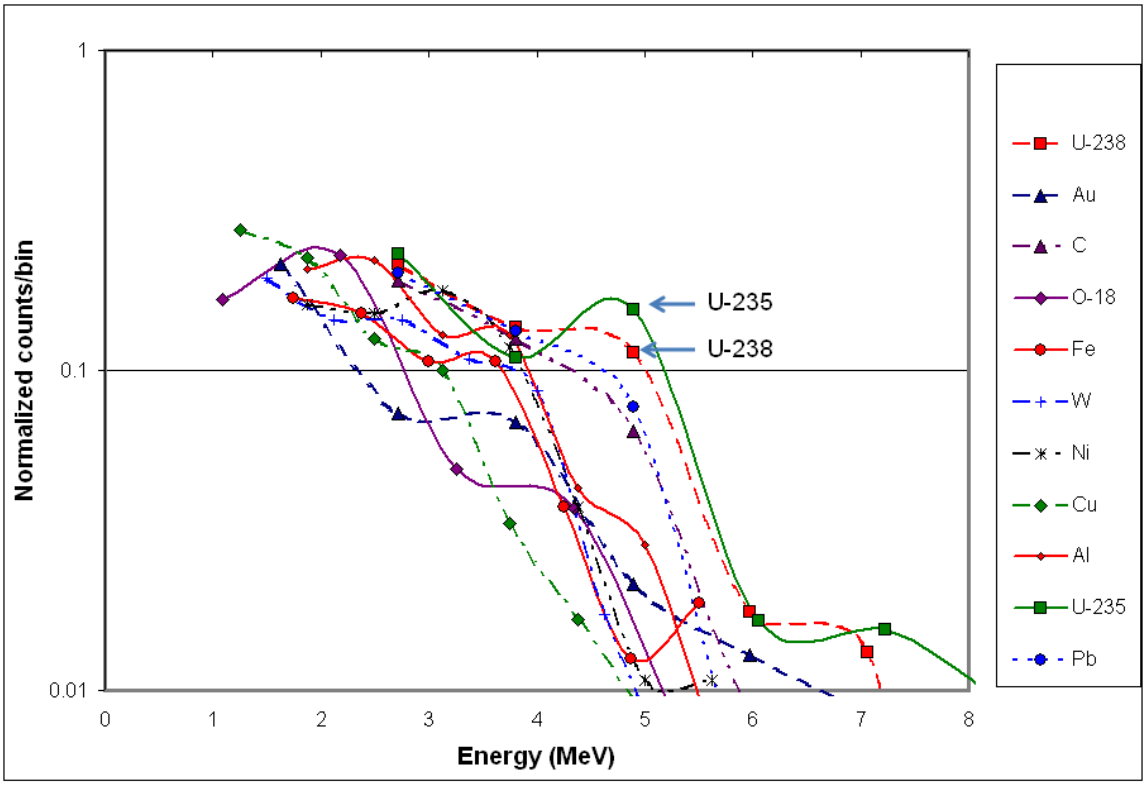
Normalized counts/bin
1
0.1
0.01
0
1
2
3
4
5
6
7
8
Energy (MeV)
U-235
U-238
U-238
Au
C
O-18
Fe
W
Ni
Cu
Al
U-235
Pb

Figure. 2.

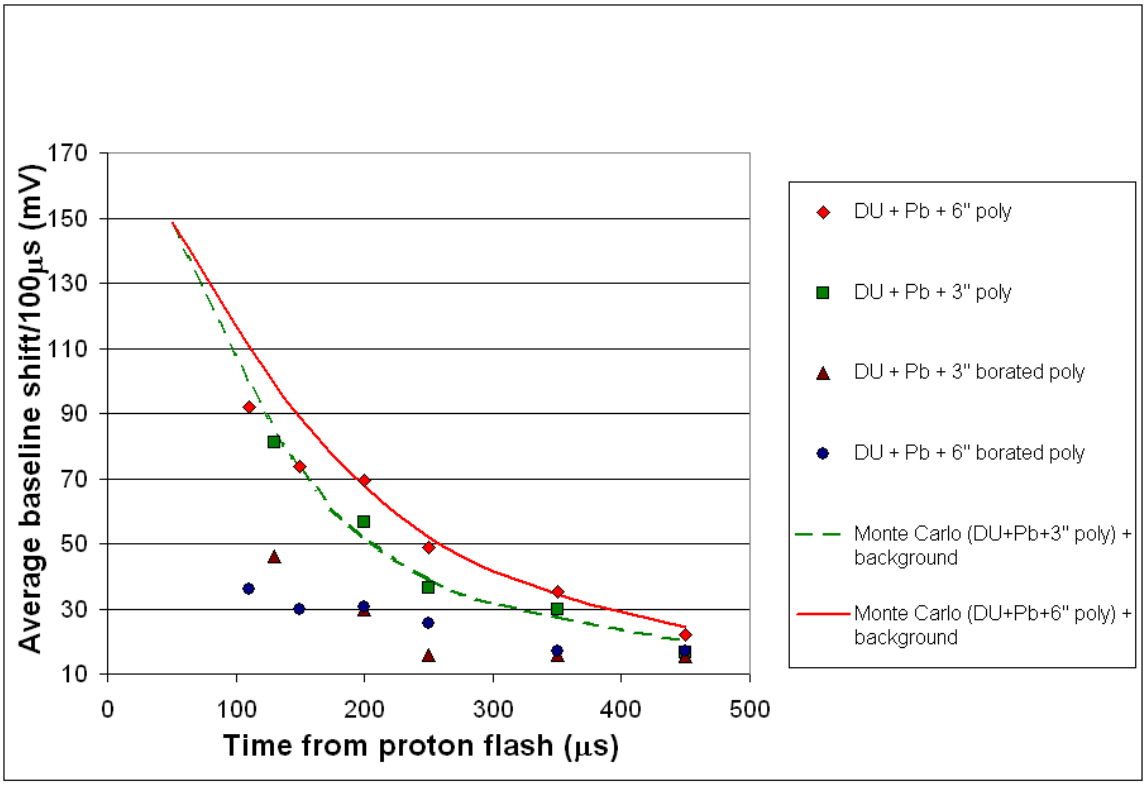
Average baseline shift/100µs (mV)
170
150
130
110
90
70
50
30
10
0
100
200
300
400
500
Time from proton flash (µs)
DU + Pb + 6" poly
DU + Pb + 3" poly
DU + Pb + 3" borated poly
DU + Pb + 6" borated poly
Monte Carlo (DU+Pb+3" poly) + background
Monte Carlo (DU+Pb+6" poly) + background

Figure 3.

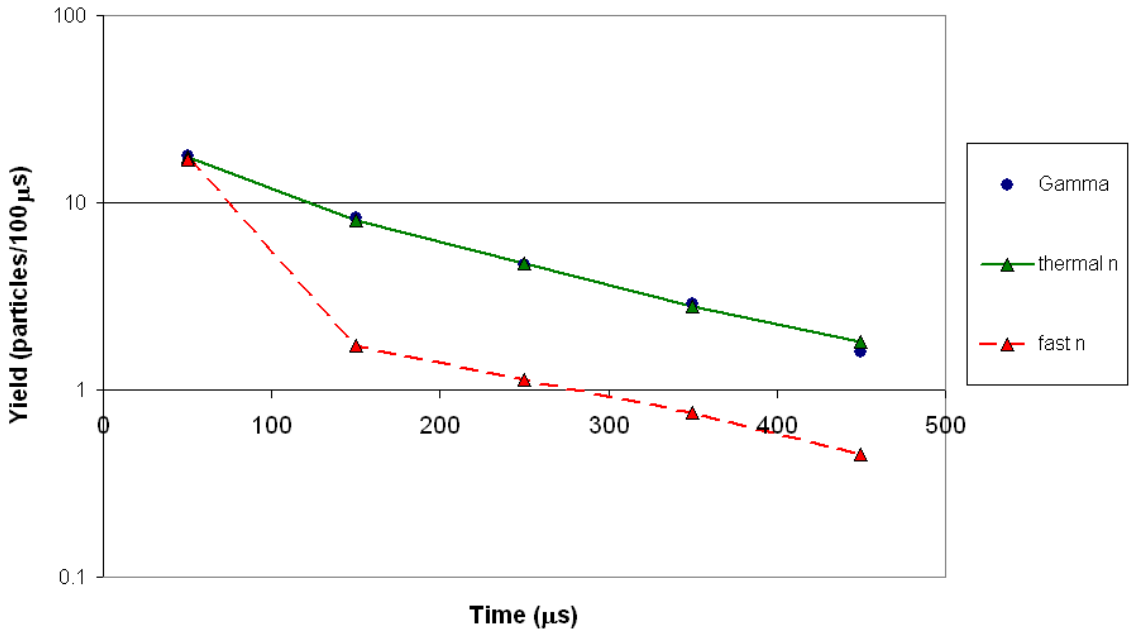
100
10
1
0.1
0
100
200
300
400
500
Yield (particles/100μs)
Time (μs)
Gamma
thermal n
fast n

Figure 4.

FIGURE CAPTIONS

Figure 1. Example of a complete recorded data set. The optical resolution is much lower than the true digital resolution recorded in the data set. In the insert, individual detected pulses are easily separated at a count rate of $2 \cdot 10^6$ counts per second.

Figure 2. Gamma ray spectra of the products of 4 GeV proton irradiations taken 350 μsec after the proton flash in a 10 μs wide time window. Note that U235/238 have the highest energy gamma rays.

Figure 3. Detected average baseline shift for DU surrounded by plain and boron loaded polyethylene (see the text for explanation.)

Figure 4. MCNPX calculation of fast and thermal neutron yields as a function of time in shielded HEU